Effect of powder characteristics on the sinterability of hydroxyapatite powders

I. R. GIBSON, S. KE, S. M. BEST, W. BONFIELD*
IRC in Biomedical Materials, Queen Mary and Westfield College, Mile End Road, London, E1 4NS, UK
E-mail: I.R.Gibson@qmw.ac.uk

The effect of different sintering conditions on the sintered density and microstructure of two different hydroxyapatite (HA) powders was examined. The powder characteristics of a laboratory synthesized HA powder (Lab HA) were low crystallinity, a bimodal particle size distribution, a median particle size of 22 μm and a high specific surface area (SSA) of 63 m^2/g. By contrast, a commercial calcined HA (commercial HA) was crystalline and had a median particle size of 5 μm and a low SSA of 16 m^2/g. The different powder characteristics affected the compactability and the sinterability of the two HA powders. Lab HA did not compact as efficiently as commercial HA, resulting in a lower green density, but the onset of sintering of powder compacts of the former was approximately 150 °C lower than the later. The effect of compaction pressure, sintering temperature, time and heating rate on the sintered densities of the two materials was studied. Varying all these sintering conditions significantly affected the sintered density of commercial HA, whereas the sintered density of Lab HA was only affected significantly by increasing the sintering temperature.

The Vickers hardness, H_v, of Lab HA was greater than commercial HA for low sintering temperatures, below 1200 °C, whereas for higher sintering temperatures the commercial HA produced ceramics with greater values of hardness. These trends can be related to the sinterability of the two materials.

1. Introduction

Hydroxyapatite (HA), $Ca_{10}(PO_4)_6(OH)_2$, is used as a biomedical material as it is biocompatible *in vivo* [1]. Clinically, HA may be used in a variety of physical forms: as a sintered ceramic, such as in granular, block or porous form [2], as a deposited coating, such as a bioactive coating on a bioinert implant [3], or as a filler phase of a polymer-ceramic composite material, such as hydroxyapatite-polyethylene, HAPEX™, implants [4]. Synthetic HA is normally prepared by either an aqueous [5, 6] or a solid state reaction route [7].

The powder properties, such as crystallinity, surface area and particle size, of the resulting HA powder will determine the effectiveness of the powder in its specific application. For example, powders with a large median particle size (~ 50 μm) are beneficial for producing HA coatings by plasma-spraying [8]. For the production of hydroxyapatite-polyethylene composites, small changes in particle size and morphology were shown to have significant effects on the mechanical properties of the composite [9].

For applications where HA powders will be sintered to form a ceramic, the mechanical properties of HA will be very dependent on the sintered density and microstructure of the final sintered product [10–17]. For the production of HA biomedical implants such as granules or porous implants, therefore, it is essential that the way in which the HA powder sinters to form a ceramic is understood. Numerous studies have examined the sinterability of HA powders that were produced by either various synthetic routes in the laboratory or commercially obtained powders [11, 13–15, 18–21]. However, it is not always easy to gain a clear correlation between the powder characteristics and the sinterability from such studies as not all the powder properties are reported, or the chemical composition of the HA materials, which has been shown to affect the sinterability [12], is not constant. For example, Fanovich and Porto Lopez [21] compared the sinterability of a commercial and synthetic HA and showed that for all sintering temperatures the sintered density of the synthetic HA was always greater than for the commercial HA. Although the particle sizes of the two powders were shown to be significantly different, the Ca/P molar ratios of the synthetic and the commercial powders were 1.77 and 1.51, respectively, which are very different to the expected value of 1.67 required for a stoichiometric, or single-phase, HA. It was not clear, therefore, which factor was affecting the sinterability of the two powders.

Several sintering or processing conditions have been

*Now at Department of Materials Science and Metallurgy, University of Cambridge, Pembroke Street, Cambridge, CB2 3QZ, UK.

reported which have resulted in the formation of fully dense HA ceramics, such as microwave sintering [22] and gel-filtration [5]. However, for conventional sintering of compacted powders, the effect of a wide range of sintering conditions, such as compaction pressure, sintering temperature, time and heating rate, on the sinterability of HA powders has not been reported. Additionally, the differences that may be observed on sintering a non-calcined synthetic HA and a calcined commercial HA have not been clearly illustrated.

The aim of this study was to compare the sinterability of a non heat-treated HA powder that was produced in the laboratory by an aqueous precipitation method with that of a commercially available calcined HA powder. The physical characteristics of the two powders were assessed fully and the effect of the different powder properties on the sintered densities of ceramics prepared under various sintering conditions was investigated. Microhardness testing was used to provide an insight into how the mechanical properties were affected by the sintered density of the different ceramics.

2. Materials and methods

2.1. Sample preparation

A stoichiometric HA (Lab HA) was prepared using the precipitation reaction between 0.5 moles calcium hydroxide, $Ca(OH)_2$ and 0.3 moles orthophosphoric acid, H_3PO_4, based on the method described by Akao *et al*. [6]. In this study, a stoichiometric HA was defined as a synthetic HA with a Ca/P molar ratio which approaches 1.67 and which, after sintering/calcining at temperatures between 800 and 1300 °C, did not decompose to form secondary phases such as TCP or CaO. The precipitation reaction was carried out at room temperature and the pH was maintained at 10.5 by the addition of ammonium hydroxide solution. After complete mixing of the reactants, the suspension was aged overnight. The resulting precipitate was filtered, dried at 80 °C overnight and then ground to a powder in a mortar and pestle. The powder was then ball milled, using a porcelain mill pot with alumina milling balls, for 1 h. The powder was then removed from the mill pot and passed through a series of sieves; as a result of this process, the maximum particle size of the final powder that was used in this study was less than 75 μm in size.

A commercial HA (commercial HA) powder (Plasma Biotal P120, UK) was used as a comparison and was studied in the as-received state.

Powder compacts were prepared by pressing uniaxially 1 g or 4 g of HA powder into a 16 mm or a 32 mm steel die, respectively. The applied load was controlled so that, irrespective of the size of die used, the pressing pressures that were used to compact the powders were the same; pressing pressures were varied between 30 and 200 MPa. The compacts were sintered in a Carbolite RHF1600 furnace at temperatures ranging from 800 to 1350 °C for times between 1–4 h, with heating rates ranging from 1–20°/min; all samples were cooled at 10°/min to room temperature.

2.2. Characterization techniques

The calcium and phosphorus contents and the level of elemental impurities of the stoichiometric HA powders were determined by X-ray fluorescence (XRF) spectroscopy using a Philips PW1606 spectrometer (Ceram Research, UK). The phase compositions of the as-prepared powders and the sintered powder compacts were analyzed by X-ray diffraction (XRD) using a Siemens D5000 diffractometer. Data were collected over the 2θ range 5–110° with a step size of 0.02° and a count time of 12 s. Identification of phases was achieved by comparing the diffraction patterns of HA with ICDD (JCPDS) standards [23].

The particle size distribution and mean particle size were measured using a Malvern Mastersizer X (Malvern Instruments, Malvern, UK). The specific surface area (SSA) of the powders was determined by the Brunauer-Emmett-Teller (BET) method using a Micromeretics Surface Area Analyzer (Department of MSE, University of Surrey, UK). Scanning electron microscopy (SEM) of the powders was performed using a JEOL 6300 SEM, which provided information about the morphology of the individual powder particles and also confirmed the particle size distribution results from PSA.

The green and sintered densities of compacts were obtained from the measurement of geometric dimensions and sample mass for low density samples ($< 95\%$ of the theoretical density) and by the water immersion method for high density samples ($> 95\%$); for low density samples, the water immersion method allows water to enter the pores, resulting in false values of the sample density. For each sintering condition, three compacts were sintered and the average value of sintered density was determined. All densities were quoted as a percentage of the theoretical density of HA, $3.156\,gcm^{-3}$ [23]. The microstructures of the sintered HA ceramics were studied using SEM. One surface of the specimen was polished to a 10 μm finish, and then etched in 10% phosphoric acid for 10 s. Prior to examination, the specimens were gold-coated to prevent charging in the microscope.

The Vickers hardness, H_v, of sintered specimens was determined using a Shimadzu microhardness indenter. A 500 g load was applied for 10 s to produce an indent. The average diagonal length of the indent was measured and this was repeated five times for each sample. The H_v was calculated from the method described in the ASTM E384 [26].

3. Results and discussion

3.1. Powder characterization

The results of the chemical analysis showed that the Ca/P molar ratio of the Lab HA was 1.68 ($\pm$ 0.01) whereas the commercial HA was 1.69 ($\pm$ 0.01). Within the accuracy of the analysis, both HA powders had Ca/P molar ratios that were comparable to that of stoichiometric HA, 1.67. The levels of impurities in the two HA powders are listed in Table I; Lab HA appeared to have significantly lower quantities of impurities than was observed for commercial HA, especially SiO_2, MgO, Al_2O_3 and Fe_2O_3.

XRD analysis showed that both Lab and commercial HA, before and after sintering, produced only peaks that

TABLE I The elemental impurities (expressed as oxides) detected by XRF analysis of Laboratory and commercial HA powders

Impurity	Laboratory HA (wt %)	Commercial HA (wt %)
SiO_2	0.04	0.34
Fe_2O_3	< 0.01	0.05
Al_2O_3	0.03	0.09
MgO	< 0.02	0.27
Na_2O	< 0.03	< 0.03

corresponded to stoichiometric HA [23]. This was further evidence that the two materials in this study were single-phase HA that did not decompose to secondary phases on sintering/heating. The only difference in the XRD patterns was in the crystallinity of the two HA powders before sintering, Fig. 1. The Lab HA was poorly crystalline, as shown by the broad diffraction peaks, which is characteristic of HA prepared by an aqueous precipitation route [24, 25]. In contrast, the as-received commercial HA powder produced a diffraction pattern that corresponded to a crystalline material, with narrow diffraction peaks, which is characteristic of a powder that has been calcined/heat-treated.

The particle size distributions of the two powders are illustrated in Fig. 2 and the values of d(0.1), d(0.5) and d(0.9), which refer to the measured particle size, or diameter, of 10, 50 and 90% of the powder particles, respectively, are listed in Table II. The Lab HA and commercial HA have bimodal particle size distributions, centered at $\sim 2\,\mu m$ and $30\,\mu m$, and at $\sim 2\,\mu m$ and $100\,\mu m$, respectively. Although the commercial HA powder consisted of a large number of very small particles, the large particles ($> 10\,\mu m$) were significantly greater in size compared to the Lab HA.

The SSA of the two powders are also listed in Table II. The small crystallites that make up the powder particles of the Lab HA results in it having a very high surface area, whereas the calcined commercial HA powder has a relatively low surface area.

The powder morphologies of the two powders are illustrated in the SEM micrographs, Fig. 3. The Lab HA (Fig. 3a) consists of a mixture of small powder particles of 1–10 μm diameter and larger, angular particles of 20–40 μm diameter. The larger particles appear to be large agglomerates of smaller particles, resulting in a rough surface, which is indicative of a high surface area. The micrograph of the commercial HA (Fig. 3b) powder reflects the smaller particle size of most of the powder particles, with most ranging between 2–5 μm. The commercial HA powder appeared to produce larger agglomerated particles, although these agglomerates appeared to be less compacted compared to those observed for Lab HA. The drying of the filter-cake of Lab HA resulted in a significant compaction of the precipitate and, although the filtercake was ground, milled and sieved, this probably resulted in the formation of hard agglomerates. Although the chemical and phase compositions of the two powders are similar, the powder properties, namely the size distribution, surface area and the morphology are very different. The different powder characteristics are largely a result of the different powder processing methods used, namely the calcination/heat-treatment of the commercial powder, and these differences should be evident in the sinterability of the two powders.

3.2. Sinterability of HA powders – compaction pressures

The effect of varying the compaction pressure (MPa) on the green density and sintered density of the two HA materials is illustrated in Fig. 4a and b, respectively. The green density of both powder compacts increased with increasing compaction pressure between 30 and 200 MPa, although the green density of commercial HA was always greater than that of Lab HA. Sintering at 1200 °C for 2 h, with a heating rate of 2.5°/min, produced a complete change in the order of the sintered densities. The Lab HA produced higher sintered densities than commercial HA for all compaction pressures, and the sintered density showed only a small increase from 94 to 98% between 30 and 200 MPa. In contrast, the sintered density of commercial HA increased steadily from a low value of only 64% for a compaction pressure of 30 MPa to a maximum of 92%

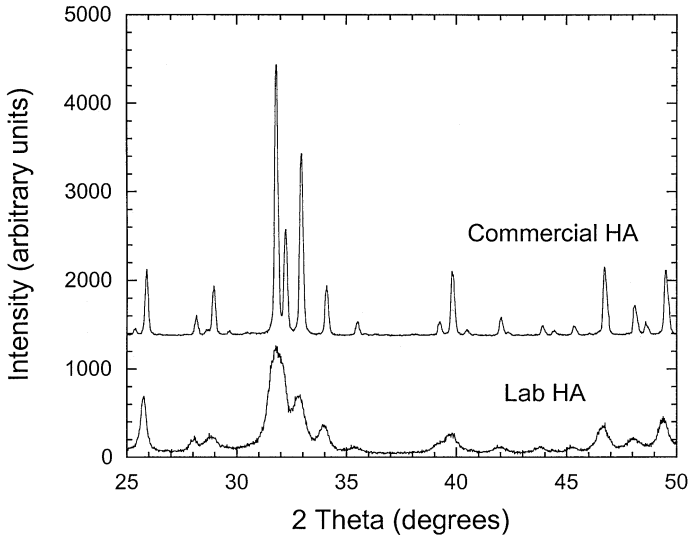

Figure 1 XRD patterns of Lab HA and commercial HA powders before sintering.

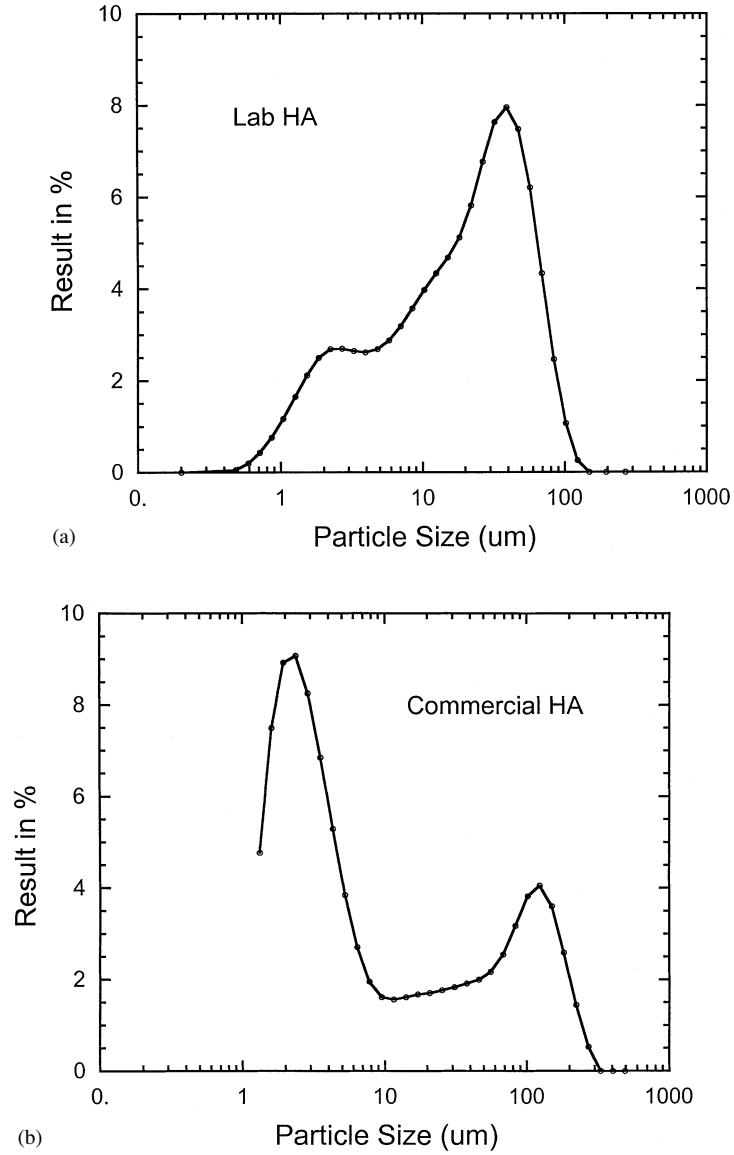

Figure 2 The particle size distributions of (a) Lab HA and (b) commercial HA powder.

for 200 MPa. Although the green density of Lab HA was less than that of commercial HA, and therefore had a lower amount of powder particle contact, Lab HA showed a much higher sinterability. This was most noticeable for the lower compaction pressures such as 30 MPa, where the green density of Lab HA was only $\sim 30\%$ compared to $\sim 40\%$ for commercial HA, whereas on sintering at 1200 °C the values reversed to 94% and 66%, respectively.

Layrolle *et al.* [20] also observed a higher green density for a commercial calcined HA than a poorly crystalline HA prepared by a $Ca(OEt)_2$ route, compacted at approximately 100 MPa, although the sintered densities showed the opposite trend to the present study, with the commercial HA also having the higher sintered density. The powder properties of the two HA materials used by Layrolle *et al.* were comparable to the powders used in this study; the lower sintered densities observed in [20] for the poorly crystalline HA prepared by a $Ca(OEt)_2$ route may be due to the large amount of organic species that must be lost during sintering/heating. Fanovich and Porto Lopez [21] compared the sinterability of a synthetic and a commercial HA which had very different particle size distributions and chemical compositions. The two materials had very similar green densities but the synthetic HA had a greater sintered density than the commercial sample. It was therefore not clear if the difference in the sinterability of the two powders was due to powder characteristics or chemical composition.

In the present study, the powder compaction pressure

TABLE II Results of surface area and particle size analysis of laboratory and commercial HA powders (d(0.1), d(0.5) and d(0.9) refer to the measured particle size, or diameter, of 10, 50 and 90% of the powder particles)

Powder	Particle size (μm)			Surface area
	d(0.1)	d(0.5)	d(0.9)	(m^2/g)
Laboratory HA	2.5	22	65	63
Commercial HA	2	5	138	13

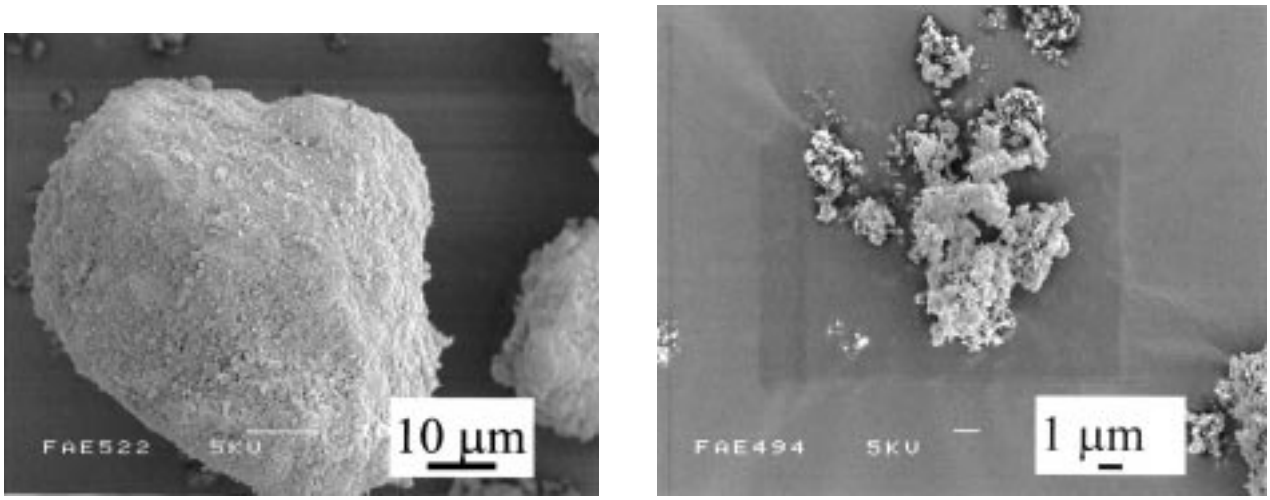

(a) (b)

Figure 3 SEM micrographs of (a) lab HA and (b) commercial HA powder.

was clearly an important variable for maximizing the sintered density of commercial HA, but did not have a major effect on Lab HA. From the results presented in Fig. 4, a compaction pressure of 200 MPa was used in all subsequent sintering trials in order to maximize the sintered densities of samples.

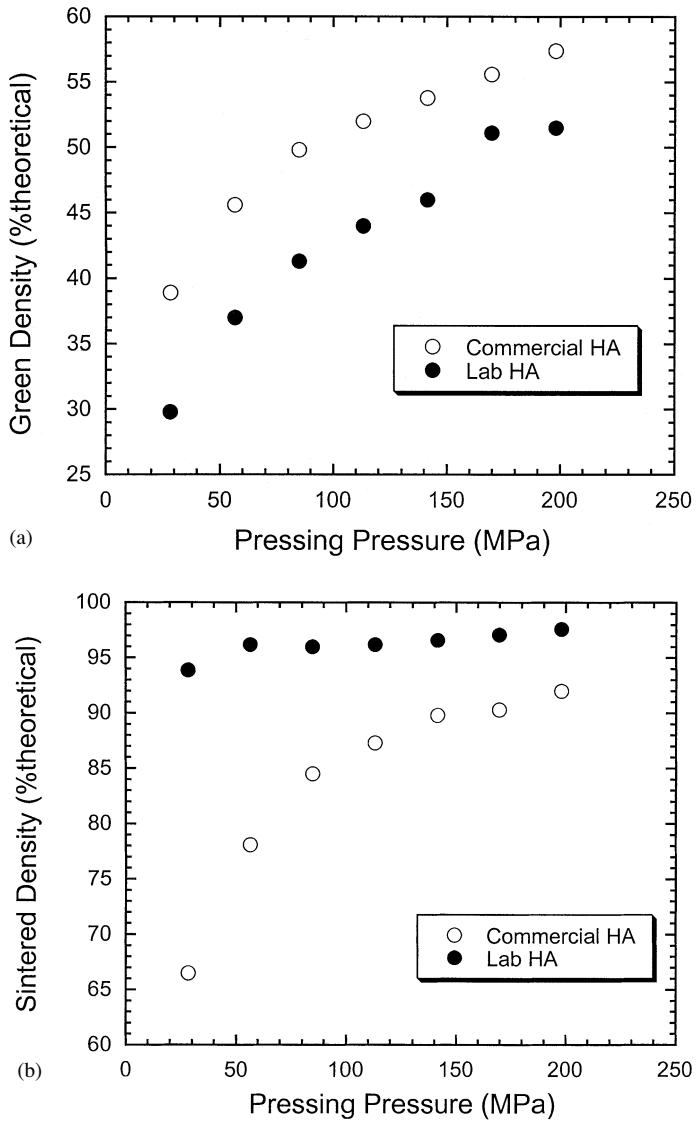

Figure 4 Effect of compaction pressure on the (a) green density and (b) sintered densities (expressed as a percentage of the theoretical density) of Lab HA and commercial HA; sintering conditions were 2.5°/min to 1200 °C for 2 h, then cooled to room temperature at 10°/min.

3.3. Sinterability of HA powders – temperature, time and heating rate

The effect of sintering temperature on the sintered densities of compacts of the two HA powders is illustrated in Fig. 5. All samples were compacted at 200 MPa, heated to the chosen sintering temperature at 2.5°/min and, after a dwell time of 2 h, cooled to room temperature at 10°/min. For a sintering temperature of 800 °C, both Lab and commercial HA had sintered densities that were comparable to their green densities, Fig. 4a. The onset of densification, indicated by a sharp increase in the sintered density, for Lab HA was between 800 and 900 °C, whereas commercial HA required a higher temperature of between 1000 and 1050 °C. This could also be illustrated by plotting the linear shrinkage of the samples as a function of sintering temperature, Fig. 6. A small increase in density is observed before the onset of densification and this corresponds to the first stage of sintering, where necks are forming between powder particles. The second stage of sintering corresponds to densification and the removal of most of the specimen porosity. For the Lab HA, this process occurs between 800 and 1050 °C, compared to 1050 and 1250 °C for commercial HA. Sintering temperatures above this range result in very small increases in density which are associated with the final stages of sintering where small levels of porosity are removed and grain growth begins. Lab HA achieves a final sintered density of between 97–98% of the theoretical density at approximately 1200 °C, whereas Commercial HA requires a sintering temperature of approximately 1300 °C to reach a similar density. The final linear shrinkages, Fig. 6, of Lab HA and commercial HA were approximately 24% and 18%, respectively. The larger shrinkage observed for the Lab HA was also associated with a decrease in sample mass on sintering of approximately 5–10%, whereas the sample mass of commercial HA remained almost constant. As the Lab HA was produced by an aqueous route and was not subjected to any heat treatment greater than drying at 80 °C, a significant amount of adsorbed water will probably remain. It is not clear if the loss of this water during sintering plays a role in the improved sinterability/densification of Lab HA, as observed in Figs 5 and 6.

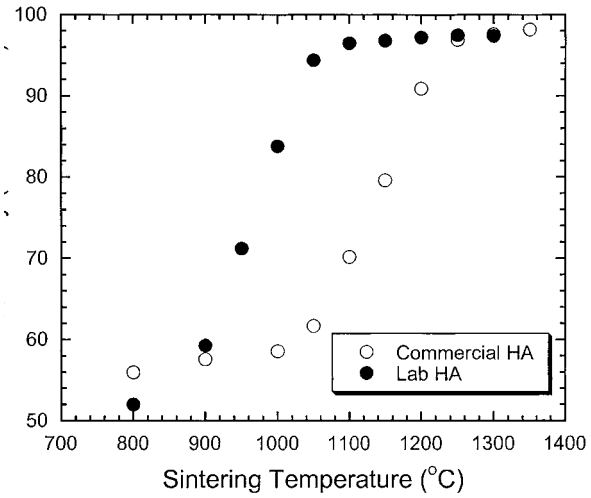

Figure 5 Effect of sintering temperature (°C) on the sintered densities (expressed as a percentage of the theoretical density) of Lab HA and commercial HA.

Two other sintering parameters that may affect the sinterability of HA powder compacts are heating rate and sintering dwell time. The effect of varying the heating rate from 1 to 20 °C/min, with a constant sintering temperature of 1200 °C and a dwell time of 2 h, on the sintered density of HA is shown in Fig. 7a. Increasing the heating rate produced a small increase in the sintered density of Lab HA, whereas the effect on commercial HA was more noticeable for rates between 1 and 5 °C/min. XRD analysis of samples that were heated at rates greater than 10 °C/min indicated that small amounts of tricalcium phosphate (TCP) were formed; this was probably a result of partial dehydroxylation due to the rapid heating rate, resulting in partial decomposition of the HA to TCP.

Increasing the sintering dwell time from between 1 to 8 h, with a constant sintering temperature of 1200 °C and a heating rate of 2.5 °C/min, also produced only small increases in the sintered densities of Lab and commercial HA, with the effect again being more significant for the latter, Fig. 7b.

The effect of different sintering conditions on the sintered densities of the two materials showed contrasting trends. Firstly, Lab HA sintered to a high density ($>$ 97% at 1200 °C) for all sintering conditions and the density was only improved by approximately 1% by varying these conditions. In contrast, commercial HA required more thermal activation, whether it was higher temperatures, longer dwell times or faster heating rates to achieve a comparable sintered density. For example, for short dwell times or slow heating rates, at 1200 °C, a sintered density of approximately 92% was achieved, and varying the sintering conditions increased the density to approximately 96%. Clearly, the Lab HA powder sinters more readily than the commercial HA and requires a much lower temperature to achieve near-theoretical density (98–99%), although for high sintering temperatures of between 1300–1350 °C the maximum sintered densities observed for both materials were comparable.

Fanovich and Porto Lopez [21] prepared HA samples, with a Ca/P = 1.77, by a similar precipitation method to that used to prepare Lab HA in this study. The HA powders that they produced were calcined at 500 and 1000 °C prior to sintering, and the sintered densities were observed to decrease with increasing calcining temperature.

To determine if the only reason that the sintered densities of Lab HA were greater than commercial HA in the present study was due to the calcining of the latter powder, samples of Lab HA were calcined at 700 to 900 °C for 1 h, and then compacted and sintered as for previous samples. The particle size of the powders was not affected by calcining, and the sintered densities of calcined Lab HA samples, sintered at 1200 °C for 2 h, were 97–98% of the theoretical density, as observed for non-calcined Lab HA, Fig. 5. Clearly, the enhanced sinterability of Lab HA compared to commercial HA was not due to Lab HA powder being non-calcined.

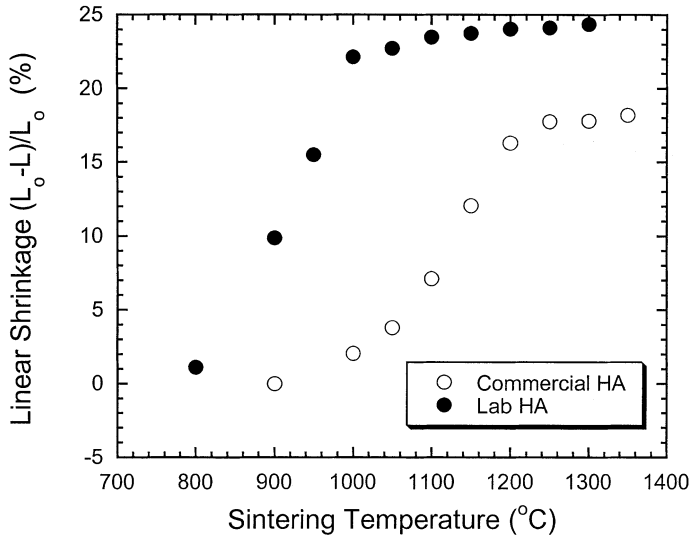

Figure 6 Linear shrinkage of Lab HA and commercial HA as a function of sintering temperature.

The effect of elemental impurities on the sinterability of the two powders could not be confirmed by this study alone. The Lab HA produced in this study had very low levels of impurities, such as SiO_2, MgO and Al_2O_3 compared to the commercial HA. The effect of different sintering additives on the sinterability of HA was reported by Suchanek *et al*. [27]. Although they did not study the effects of SiO_2, MgO or Al_2O_3, they did demonstrate that additives could significantly affect the sinterability of HA.

3.4. Sinterability of HA powders – ceramic microstructures

SEM images of Lab HA and commercial HA, sintered at 1000, 1100 and 1250 °C are presented in Fig. 8a–f. At 1000 °C, the powder particles of Lab HA are clearly beginning to sinter together, with some areas of large agglomerates (approximately 10–20 μm) forming dense regions, Fig. 8a. The powder particles of commercial HA, by contrast, have not started to sinter together, and the microstructure at 1000 °C, Fig. 8b, is comparable to the green body. Commercial HA requires a sintering temperature of 1100 °C, Fig. 8d, to achieve a microstructure that is comparable to Lab HA at 1000 °C. At 1100 °C, Lab HA has a dense microstructure composed of grains that are approximately 1 μm in size and a small level of porosity. For a higher sintering temperature of 1250 °C, Lab HA and commercial HA exhibit significant grain growth, with some grains reaching approximately 5 μm in size. The microstructures of the two materials are quite similar at higher temperatures, where near-theoretical densities are obtained, with the grain sizes ranging between 1 and 5 μm.

3.5. Vickers hardness

The effect of sintering temperature on the Vickers hardness, H_v, of Lab HA and commercial HA is represented in Fig. 9; a heating rate of 2.5 °C/min and a dwell time of 2 h was used for all samples. Commercial HA shows no significant change in hardness over the temperature range 900–1100 °C, whereas Lab HA shows a large increase in hardness from 900 to 1000–1100 °C.

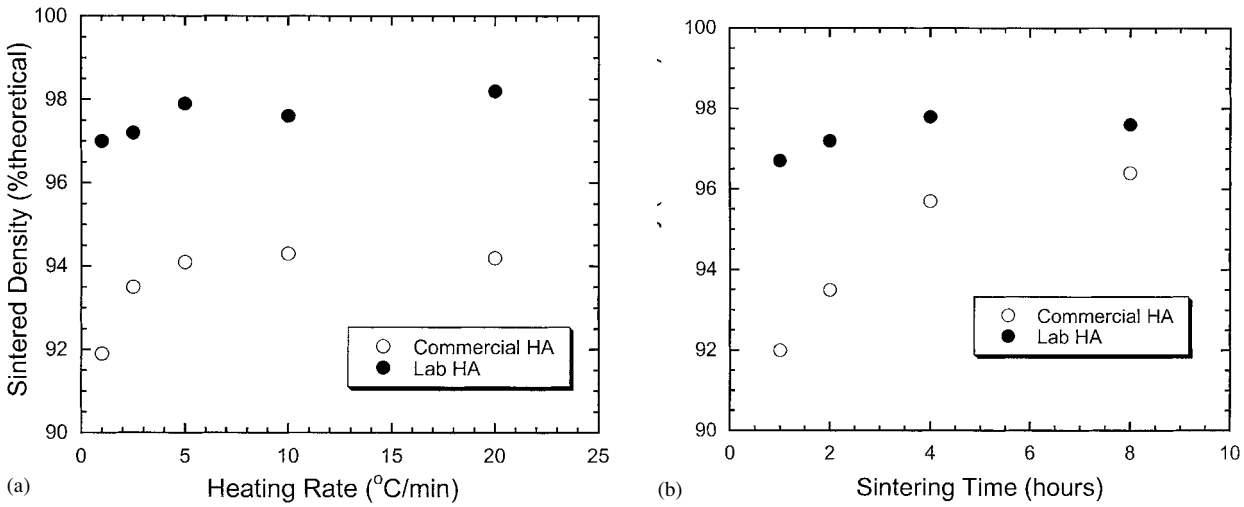

Figure 7 Effect of (a) heating rate (°C/min) and (b) sintering dwell time on the sintered densities of Lab HA and commercial HA; for all conditions the sintering temperature was 1200 °C.

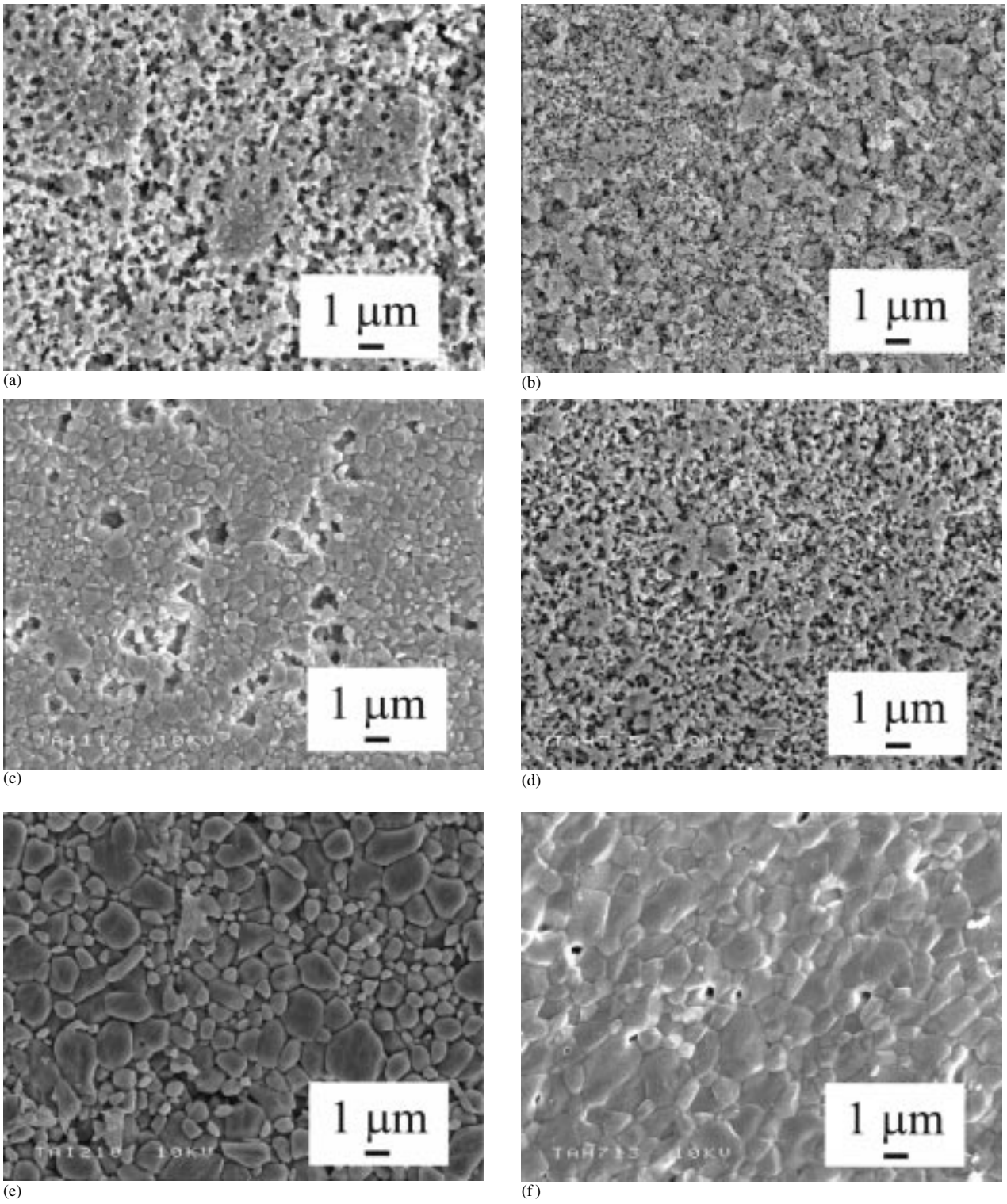

Figure 8 SEM images of Lab HA and commercial HA sintered at (a and b) 1000 °C, (c and d) 1100 °C and (e and f) 1250 °C, respectively.

From the data obtained for the effect of sintering temperature on the sintered densities of the samples, Fig. 5, Lab HA showed a rapid increase in density from 58% at 900 °C to 84 and 96.5% at 1000 °C and 1100 °C, respectively. This increase in density is reflected in the improved hardness with increased sintering temperature, whereas the sintered density and hardness of commercial HA showed only a small increase over this temperature range. The Lab HA samples sintered at 1200–1250 °C continued to show a small increase in hardness, whereas the commercial HA showed a sudden increase in hardness for samples sintered from 1100 to 1200–1250 °C. Again, from the results presented in Fig. 5, the sintered density of Lab HA increases by only 1–2% over this temperature range, whereas the density of commercial HA increases from 70% at 1100 °C to 91 and 97% at 1200 and 1250 °C, respectively. The hardness results show clearly the effect of sintered density on the hardness of HA ceramics, and that the hardness of Lab HA is greater than commercial HA for lower sintering temperatures, where it achieves higher sintered densities. The results obtained in this study are not comparable to the results reported by Wang and Chaki [11] for the effect of sintering temperature on the Knoop hardness of a synthetic HA; Wang and Chaki demonstrated that the hardness reached a large maxima for sintering tempera-

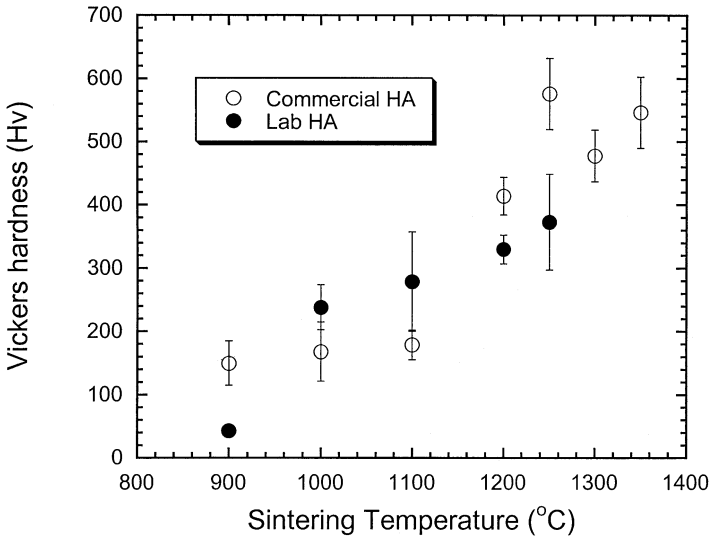

Figure 9 Effect of sintering temperature on the Vickers hardness of Lab HA and commercial HA.

tures between 1100 and 1200 °C. This trend related to the sintered densities observed in their study, where the density reached a maximum between 1100 and 1200 °C before decreasing with increasing sintering temperature. Van Landuyt *et al*. [16] studied the effects of sintering temperature (1200 to 1450 °C) on the Vickers hardness of a commercial HA, and their results showed a similar trend to the commercial HA in this study, for temperatures between 1200 and 1350 °C.

4. Conclusions

The sinterability of a high purity, single-phase HA powder (Lab HA), which was produced in this study by an aqueous precipitation reaction, was significantly greater than for a commercial, calcined HA powder (commercial HA). The temperature for the onset of sintering and the temperature required to achieve near-theoretical density were approximately 150–200 °C lower for Lab HA than commercial HA. Only the sintering temperature significantly affected the sintered density of Lab HA, whereas the sintering temperature, time, heating rate and compaction pressure all affected the sintered density of commercial HA. The enhanced sinterability of the Lab HA was probably due to a higher level of chemical purity and better powder characteristics, compared to commercial HA. The effect of sintering temperature on the sintered densities of the two materials was reflected in the Vickers hardness values.

Acknowledgments

The support of the Engineering and Physical Sciences Research Council for funding of the IRC in Biomedical Materials is gratefully acknowledged. The authors would also like to thank Mr John Merry for his assistance with the Vickers hardness measurements.

References

1. A. MORONI, V. L. CAJA, E. L.EGGER, L. TRINCHESE and E. Y. S. CHAO, *Biomaterials* **15** (1994) 926.
2. T. KOBAYASHI, S. SHINGAKI, T. NAKAJIMA and K. HANADA, *J. Long-Term Effects of Med. Impl.* **3** (1993) 283.
3. J. D. DE BRUIJN, Y. P. BOVELL and C. A. VAN BLITTERSWIJK, *Biomaterials* **15** (1994) 543.
4. W. BONFIELD, M. D. GRYNPAS, A. E. TULLY, J. BOWMAN and J. ABRAM, *Biomaterials* **2** (1981) 185.
5. M. JARCHO, C. H. BOLEN, M. B. THOMAS, J. BOBICK, J. F. KAY and R. H. DOREMUS, *J. Mater. Sci.* **11** (1976) 2027.
6. M. AKAO, H. AOKI and K. KATO, *ibid.* **16** (1981) 809.
7. T. S. B. NARASARAJU, V. L. N. RAO, M. LAL and U. S. RAI, *Indian J. of Chem.* **13** (1975) 369.
8. K. A. GROSS and C. C. BERNDT, *J. Biomed. Mat. Res.* **39** (1998) 580.
9. M. WANG, R. JOSEPH and W. BONFIELD, *Biomaterials* **19** (1998) 2357.
10. W. R. RAO and R. F. BOEHM, *J. Dent. Res.* **53** (1974) 1351.
11. P. E. WANG and T. K. CHAKI, *J. Mater. Sci.* **4** (1993) 150.
12. A. ROYER, J. C. VIGUIE, M. HEUGHEBAERT and J. C. HEUGHEBAERT, *J. Mater. Sci.: Mater. Med.* **4** (1993) 76.
13. S. BEST and W. BONFIELD, *ibid.* **5** (1994) 516.
14. S. PUAJINDANETR, S. BEST and W. BONFIELD, *Brit. Ceram. Trans.* **93** (1994) 96.
15. M. G. S. MURRAY, J. WANG, C. B. PANTON and P. M. MARQUIS, *J. Mater. Sci.* **30** (1995) 3061.
16. P. VAN LANDUYT, F. LI, J. P. KEUSTERMANS, J. M. STREYDIO, F. DELANNAY and E. MUNTING, *J. Mater. Sci.: Mater. Med.* **6** (1995) 8.
17. A. J. RUYS, M. WEI, C. C. SORRELL, M. R. DICKSON, A. BRANDWOOD and B. K. MILTHORPE, *Biomaterials* **16** (1995) 409.
18. A. J. RUYS, C. C. SORRELL, A. BRANDWOOD and B. K. MILTHORPE, *J. Mater. Sci. Lett.* **14** (1995) 744.
19. H. M. ROOTARE and R. G. CRAIG, *J. Oral. Rehab.* **5** (1978) 293.
20. P. LAYROLLE, A. ITO and T. TATEISHI, *J. Am. Ceram. Soc.* **81** (1998) 1421.
21. M. A. FANOVICH and J. M. PORTO LOPEZ, *J. Mater. Sci.: Mater. Med.* **9** (1998) 53.
22. Y. FANG, D. K. AGRAWAL, D. M. ROY and R. ROY, *J. Mater. Res.* **9** (1994) 180.
23. PDF Card no. 9–432, ICDD, Newton Square, Pennsylvania, USA.
24. A. OSAKA, Y. MIURA, K. TAKEUCHI, M. ASADA and K. TAKAHASHI, *J. Mater. Sci.: Mater. Med.* **2** (1991) 51.
25. I. R. GIBSON, S. M. BEST and W. BONFIELD, *J. Biomed. Mat. Res.* **44** (1999) 422.
26. ASTM E 384–84 Standard test method for microhardness of materials. ASTM Committee on Standards, Philadelphia, USA.
27. W. SUCHANEK, M. YASHIMA, M. KAKIHANA and M. YOSHIMURA, *Biomaterials* **18** (1997) 923.

Received 1 July 1999
and accepted 24 August 1999